Field re-entrant hidden-order phase under pressure in URu_2Si_2

2010 J. Phys.: Condens. Matter 22 164205

(http://iopscience.iop.org/0953-8984/22/16/164205)

J. Phys.: Condens. Matter **22** (2010) 164205 (4pp) doi:10.1088/0953-8984/22/16/164205

Field re-entrant hidden-order phase under pressure in URu_2Si_2

D Aoki, F Bourdarot, E Hassinger, G Knebel, A Miyake, S Raymond, V Taufour and J Flouquet

INAC/SPSMS, CEA-Grenoble, 17 rue des Martyrs, F-38054 Grenoble, France

E-mail: dai.aoki@cea.fr

Received 17 June 2009, in final form 11 January 2010
Published 30 March 2010
Online at stacks.iop.org/JPhysCM/22/164205

Abstract
We succeeded in growing high quality single crystals of URu_2Si_2 and performed thermal expansion measurements under pressure. Applying a magnetic field along the [001] direction in the tetragonal structure, the so-called hidden-order phase reappears after the suppression of the antiferromagnetic phase above the critical pressure P_x. We determined the pressure–temperature–field phase diagram for the paramagnetic, hidden-order and antiferromagnetic states for the $H \parallel [001]$ direction. We also present the temperature dependence of the upper critical field H_{c2} for $H \parallel [001]$ and [100] determined by the AC specific heat measurements, corresponding to the bulk superconductivity in a high quality single crystal.

(Some figures in this article are in colour only in the electronic version)

URu_2Si_2 has attracted much attention since the so-called hidden-order (HO) state below $T_0 = 17.5$ K was mysteriously detected more than 20 years ago. Previous pressure studies have demonstrated that the antiferromagnetic (AF) state starts to develop above $P_x \simeq 0.5$ GPa [1, 2]. Now it has been clarified that Fermi surface reconstruction with a large drop in carrier numbers occurs at T_0. The neutron scattering experiments showed that the HO phase is characterized by a resonance at an energy of $E_0 \sim 2$ meV for the wavevector $\boldsymbol{Q}_0 = (1, 0, 0)$. In the AF phase, the resonance at $\boldsymbol{Q}_0$ disappears, while the higher energy excitation at the incommensurate wavevector $\boldsymbol{Q}_1 = (1.4, 0, 0)$ persists in the AF state [3]. In order to clarify the HO and AF states, we have grown high quality single crystals of URu_2Si_2 and measured the thermal expansion under high pressure by tuning the magnetic field [4].

High quality single crystals of URu_2Si_2 were grown by the Czochralski method. The starting materials of U (purity: 99.9%, 3N), Ru (4N) and Si (6N) with stoichiometric amounts were melted. The single crystals were pulled at a speed of 15 mm h^{-1} under pure Ar atmosphere gas in a tetra-arc furnace. The single crystal oriented along the [001] direction was used as a seed in order to grow the large cylindrical-shaped single crystal directed along the [001] direction for the inelastic neutron scattering experiments under pressure. As shown in figure 1, a large single crystal 70 mm in length and 7 mm in maximum diameter was successfully grown. The single crystals were oriented by x-ray Laue photography and were cut by a spark cutter. The samples are annealed at 1075 °C for 5 days under ultrahigh vacuum. The thermal expansion was measured by the so-called active-dummy method, using a strain gauge in a CuBe–NiCrAl hybrid pressure cell with Daphne oil 7373 as a pressure medium. The strain gauge was glued on the (001) plane of the sample with dimensions of $2 \times 2 \times 0.5$ mm^3. The thin sample allowed us to detect the sharp transitions at T_0 and T_x between HO and AF, and T_N between the AF and paramagnetic (PM) state, since the pressure inhomogeneity in the sample is expected to be small in the pressure cell. The AC specific heat at ambient pressure was measured by using an AuFe–Au thermocouple. The Shubnikov–de Haas (SdH) experiments were done by the four-

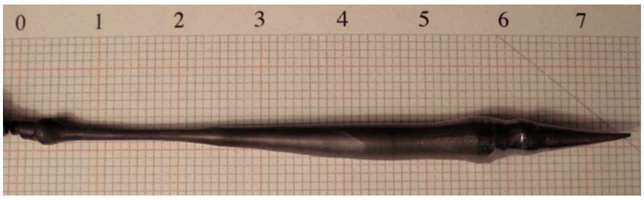

Figure 1. Photograph of a high quality single crystal URu_2Si_2 grown by the Czochralski method.

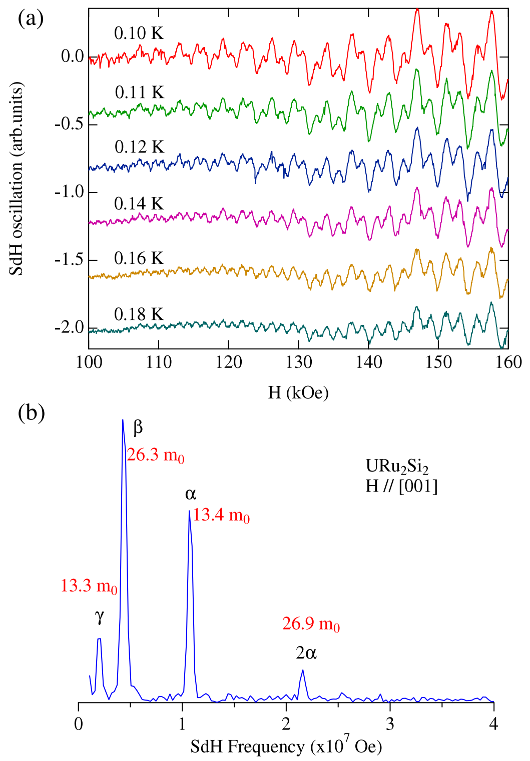

Figure 2. (a) Shubnikov–de Haas (SdH) oscillations and (b) the corresponding FFT spectrum at 0.10 K for $H \parallel [001]$ in URu_2Si_2 at ambient pressure. The red annotations in the bottom panel are the cyclotron masses obtained from the temperature dependence of the SdH amplitude.

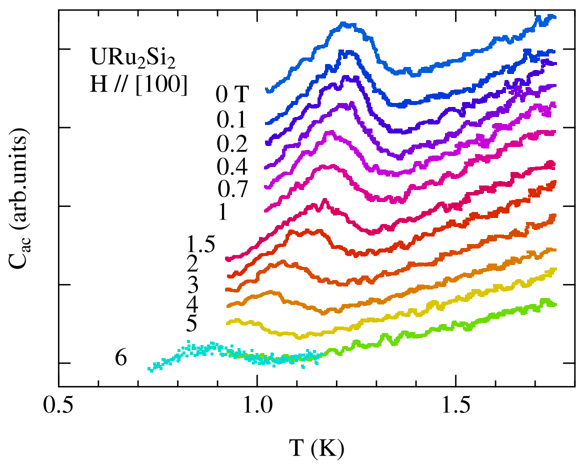

Figure 3. Temperature dependence of the AC specific heat under magnetic fields for $H \parallel [100]$ in URu_2Si_2. The data are vertically shifted for clarity.

probe AC method for the electrical current along [100] and for $H \parallel [001]$ up to 16 T, at low temperatures down to 0.1 K. The quality of all samples was checked by the resistivity measurements. The residual resistivity ratios are more than 100, indicating the high quality of the present samples.

The SdH signal clearly demonstrates that the present sample is of high quality, as shown in figure 2. From the fast Fourier transform (FFT) analysis, we detected three kinds of branches, namely α, β and γ, together with the second harmonics of branch α. It is noted that the frequency is proportional to the extremal cross-sectional area S_F, namely $F = \hbar c S_F / 2\pi e$. The detected frequencies for $H \parallel [001]$ are almost the same as the previous results [5], in which the frequencies for branches α, β and γ are found to be almost invariant against the field angle, indicating the existence of closed spherical Fermi surfaces. Assuming the spherical Fermi surfaces in the magnetic Brillouin zone with $\boldsymbol{Q}_{AF} = (0, 0, 1)$, the volumes of Fermi surfaces corresponding to branches α, β and γ occupy 1.6, 0.4 and 0.1%, respectively. The cyclotron masses m_c^* are determined by the temperature dependence of the amplitude, following the Lifshitz–Kosevich formula. The masses are $13.4m_0$, $26.3m_0$ and $13.3m_0$ for branches α, β and γ, respectively. From these values, we can simply estimate the contribution to the electronic specific heat coefficient (γ value). For the spherical Fermi surface, the γ value is simply written as [6]

$$\gamma = \frac{\pi^2}{3} k_B^2 D(\varepsilon_F), \tag{1}$$

$$D(\varepsilon_F) = \frac{V}{2\pi^2} \left(\frac{2m_c^*}{\hbar^2} \right)^{3/2} \varepsilon_F^{1/2}, \tag{2}$$

where $D(\varepsilon_F)$ and V are the density of state and the molar volume, respectively. The calculated γ values are 6.2, 7.8 and 2.7 mJ $K^{-2}mol^{-1}$ for branches α, β and γ, respectively. The sum of the calculated γ value should be equal to the γ value obtained by the specific heat experiments. On the other hand, the specific heat experiments reveal $\gamma = 55$ mJ K^{-2} mol^{-1}. Thus there should be undetected Fermi surfaces with large cyclotron masses. Of course, the sum of the calculated γ value depends on the number of Fermi surfaces in the Brillouin zone, that is, it depends on the position of the Fermi surface in the Brillouin zone. Furthermore, the volume of electron and hole Fermi surfaces must compensate each other, since URu_2Si_2 is a low carrier system. From branches α, β and γ, it is difficult to reconcile both the γ value and the carrier compensation. It is noted that the undetected heavy Fermi surface is also suggested by the recent thermal conductivity measurements [7].

Figure 3 shows the temperature dependence of the AC specific heat under magnetic fields for $H \parallel [100]$. Clear jumps due to the superconducting transition were detected. At zero field, T_c defined as the middle point of a jump is equal to 1.3 K, which is almost the same as the previous results of specific heat measurements with the high quality sample [8]. The value of T_c detected by specific heat is always lower than that detected by resistivity measurements. With magnetic fields, T_c shifts to the lower temperatures.

We also measured the AC specific heat for $H \parallel [001]$. From both temperature dependence and field dependence of the AC specific heat, the H_{c2} phase diagram was determined, as shown in figure 4. The present results are similar to the previous results determined by the resistivity measurements, although T_c and H_{c2} are slightly lower than the resistivity results. This is natural because the AC specific heat detects the bulk superconductivity, while the resistivity becomes zero even by the filamentary superconductivity. The initial slopes of H_{c2}, namely $-dH_{c2}/dT$ at T_c, are 11 and 18 T K^{-1} for $H \parallel [001]$ and [100], respectively. These values are larger

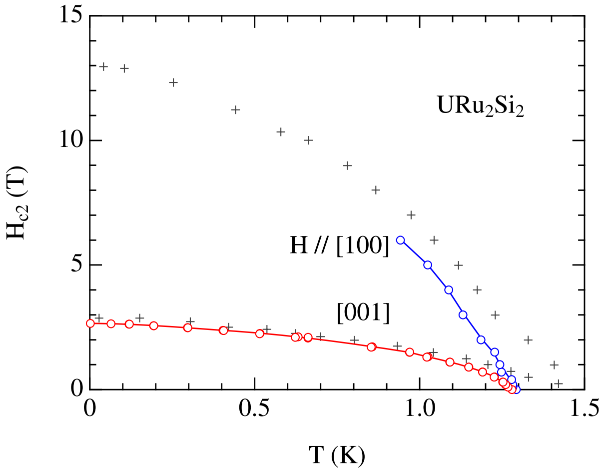

Figure 4. Temperature dependence of the upper critical fields H_{c2} for $H \parallel$ [001] and [100] in URu_2Si_2 determined by the AC specific heat. The cross symbols are cited from the previous report by resistivity measurements [5].

than those obtained from the resistivity measurements [5, 9], because the resistivity measurements close to T_c always show a strong upward curvature, which depends on the quality of the sample. The anisotropy of the initial slope may indicate the anisotropy of the effective mass or Fermi velocity, since the initial slope is governed by the orbital limit.

In order to clarify the interplay between the HO and AF state, we measured the thermal expansion. Figure 5 shows the temperature dependence of the thermal expansion coefficient along the [100] direction at various fields for $H \parallel$ [001]. At 0.56 GPa, small anomalies caused by the phase transition from PM to HO are detected at T_0, which is slightly shifted to the lower temperature with field. At higher pressure, 1.39 GPa, the large jumps corresponding to the transitions from PM to AF are observed at low fields. In addition, the small jump appears above 5 T. With increasing field, the small jump is clearly separated from the large anomaly, indicating that HO reappears after suppression of AF by the magnetic field. At 1.70 GPa, only large jumps due to the AF transition are observed although the width of the transition is large compared to that at 1.39 GPa at 9 T, suggesting that the hidden-order transition may degenerate into the antiferromagnetic transition.

The corresponding field–temperature phase diagrams are shown in figure 6. The dotted lines are obtained from the results of scaling for various pressures. At low pressures, the only HO phase appears at low temperatures. The AF phase is observed at high pressure. Compared to the HO transition, the AF transition is not robust against the field. Thus the HO phase reappears under magnetic fields. It is noted that the similar field re-entrant HO phase is reported in the Rh-doped compound $U(Ru_{0.98}Rh_{0.02})_2Si_2$, which is expected to be the case of chemical pressure [10].

We measured the thermal expansion under fields at 11 different pressures. The schematic pressure–temperature–field phase diagram is shown in figure 7, as a summary. The field where the AF phase is suppressed at 0 K, namely $H_{AF}(T = 0)$, increases with increasing pressure. On the other hand, the field where the HO phase collapses at 0 K, namely $H_M(0)$, also increases with pressure, but more moderately increases compared to $H_{AF}(0)$. It is interesting to study $H_{AF}(0)$ and $H_M(0)$ at high pressure above 2 GPa, which is left for future study.

It is worthwhile noting that in the usual antiferromagnet the field-induced ferromagnetic state (paramagnetic state) is realized above $H_{AF}(0)$, corresponding to the spin flip of the sublattice moment. On the other hand, in URu_2Si_2, the HO phase appears above $H_{AF}(0)$, where the sublattice magnetization goes from $M_0 \sim 0.3\ \mu_B$ to zero with increasing field, indicating that $H_{AF}(0)$ is not a metamagnetic transition.

According to the previous dHvA experiments, the Fermi surface detected as branch α is unchanged from HO to AF, but effective masses decreases monotonically [11]. We now succeeded in measuring three dHvA branches α, β and γ both

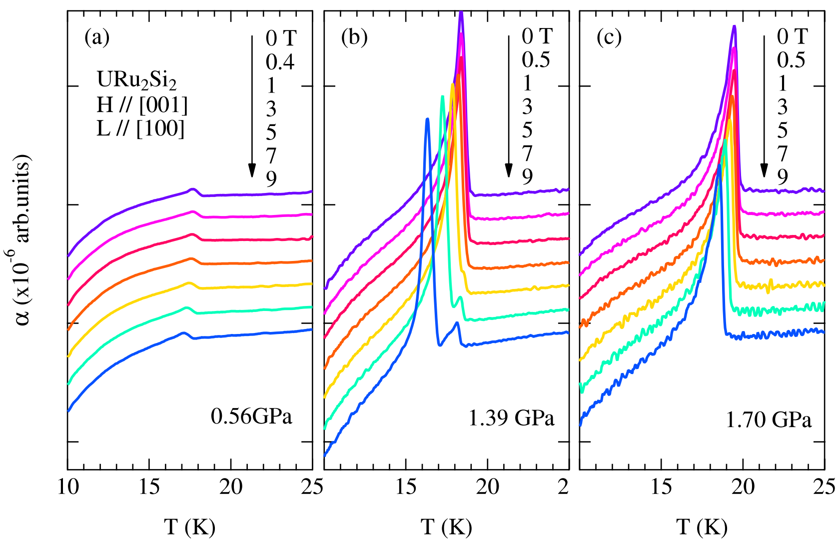

Figure 5. Temperature dependence of the thermal expansion measurements under magnetic fields at 0.56, 1.39 and 1.70 GPa in URu_2Si_2. The data are vertically shifted for clarity.

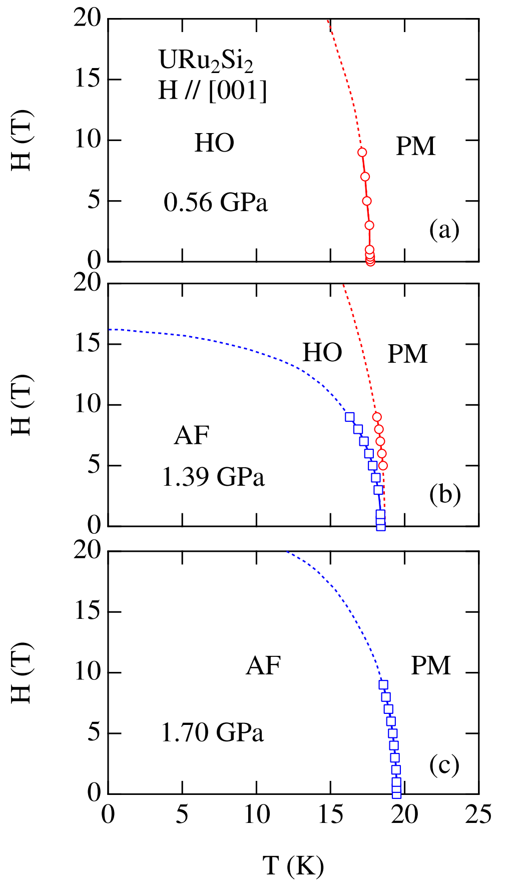

Figure 6. Field–temperature phase diagram at 0.56, 1.39 and 1.70 GPa in URu_2Si_2. PM, HO and AF denote paramagnetic, hidden-order and antiferromagnetic phase, respectively. The dotted lines are the results of scaling from the various pressures.

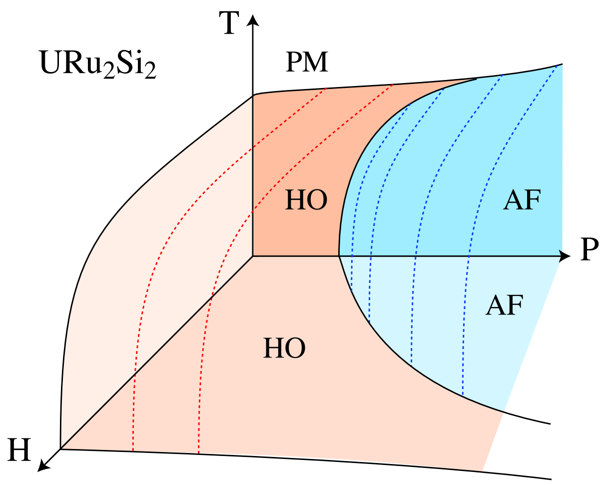

Figure 7. Schematic temperature–pressure–field phase diagram of URu_2Si_2.

below and above P_x. As they remains unchanged, the Fermi surface in AF seems to be the same as that in HO, suggesting the Fermi surface reconstruction at T_0 and T_N. This is a second indication that the HO wavevector may be the same as the AF wavevector. The details will be published elsewhere.

In summary, we have measured the thermal expansion under pressure by tuning the magnetic field with high quality single crystals. The large and small jumps due to the HO and AF transitions, respectively, were clearly detected. Above P_x, the AF phase is suppressed by the magnetic field, while the HO phase is more robust. Consequently, the re-entrant HO phase was observed with increasing field. The H_{c2} phase diagram corresponding to the bulk superconductivity was also presented by the AC specific heat measurement. The interesting point is the difference in the temperature dependence of H_{c2} for $H \parallel$ [001] and [100]. For $H \parallel$ [001], H_{c2} is limited by the Pauli limit at low temperature while for $H \parallel$ [100], the Pauli limit plays a minor role. The unusual H_{c2} curve for $H \parallel$ [100] may be linked to the microscopic nature of the HO phase.

Acknowledgment

This work was financially supported by the French ANR project ECCE and CORMAT.

References

[1] Amitsuka H, Matsuda K, Kawasaki I, Tenya K, Yokoyama M, Sekine C, Tateiwa N, Kobayashi T C, Kawarazaki S and Yoshizawa H 2007 *J. Magn. Magn. Mater.* **310** 214–20

[2] Hassinger E, Knebel G, Izawa K, Lejay P, Salce B and Flouquet J 2008 *Phys. Rev.* B **77** 115117

[3] Villaume A, Bourdarot F, Hassinger E, Raymond S, Taufour V, Aoki D and Flouquet J 2008 *Phys. Rev.* B **78** 012504

[4] Aoki D, Bourdarot F, Hassinger E, Knebel G, Miyake A, Raymond S, Taufour V and Flouquet J 2009 *J. Phys. Soc. Japan* **78** 053701

[5] Ohkuni H, Inada Y, Tokiwa Y, Sakurai K, Settai R, Honma T, Haga Y, Yamamoto E, Ōnuki Y, Yamagami H, Takahashi S and Yanagisawa T 1999 *Phil. Mag.* B **79** 1045

[6] Aoki D, Wiśniewski P, Miyake K, Watanabe N, Inada Y, Settai R, Yamamoto E, Haga Y and and Ōnuki Y 2000 *Phil. Mag.* B **80** 1517–44

[7] Kasahara Y, Iwasawa T, Shishido H, Shibauchi T, Behnia K, Haga Y, Matsuda T D, Onuki Y, Sigrist M and Matsuda Y 2007 *Phys. Rev. Lett.* **99** 116402

[8] Yano K, Sakakibara T, Tayama T, Yokoyama M, Amitsuka H, Homma Y, Miranović P, Ichioka M, Tsutsumi Y and Machida K 2008 *Phys. Rev. Lett.* **100** 017004

[9] Brison J P, Keller N, Vernière A, Lejay P, Buzdin L S A, Flouquet J, Julian S R and Lonzarich G G 1995 *Physica* C **250** 128

[10] Bourdarot F, Fåk B, Lapierre F, Sheikin I and Lejay P 2005 *Physica* B **359–361** 1132

[11] Nakashima M, Ohkuni H, Inada Y, Settai R, Haga Y, Yamamoto E and Ōnuki Y 2003 *J. Phys.: Condens. Matter* **15** S2011